



Deformation forecasting of a hydropower dam by hybridizing a long short-term memory deep learning network with the coronavirus optimization algorithm

Kien-Trinh T. Bui¹ | José F. Torres² | David Gutiérrez-Avilés² |
Viet-Ha Nhu³ | Dieu Tien Bui⁴ | Francisco Martínez-Álvarez²

¹ Faculty of Water Resources Engineering, Thuyloi University, Hanoi, Vietnam

² Data Science and Big Data Lab, Pablo de Olavide University, ES-41013 Seville, Spain

³ Department of Geological-Geotechnical Engineering, Hanoi University of Mining and Geology, Hanoi, Vietnam

⁴ GIS Group, Department of Business and IT, University of South-Eastern Norway, Bø i Telemark, Norway

Correspondence

Kien-Trinh T. Bui, Faculty of Water Resources Engineering, Thuyloi University, Hanoi, Vietnam

Email: bktrinh@tlu.edu.vn

Francisco Martínez-Álvarez, Data Science and Big Data Lab, Pablo de Olavide University, ES-41013 Seville, Spain.

Email: fmaralv@upo.es

Funding information

Vietnam National Foundation for Science and Technology Development (NAFOSTED), Grant Number: 105.08-2018.06; Spanish Ministry of Science, Innovation and Universities under project, Grant Number: PID2020-117954RB-C21.

<https://doi.org/10.1111/mice.12810>

Abstract

The safety operation and management of hydropower dam play a critical role in social-economic development and ensure people's safety in many countries; therefore, modeling and forecasting the hydropower dam's deformations with high accuracy is crucial. This research aims to propose and validate a new model based on deep learning long short-term memory (LSTM) and the coronavirus optimization algorithm (CVOA), named CVOA-LSTM, for forecasting the deformations of the hydropower dam. The second-largest hydropower dam of Vietnam, located in the Hoa Binh province, is focused. Herein, we used the LSTM to establish the deformation model, whereas the CVOA was utilized to optimize the three parameters of the LSTM, the number of hidden layers, the learning rate, and the dropout. The efficacy of the proposed CVOA-LSTM model is assessed by comparing its forecasting performance with state-of-the-art benchmarks, sequential minimal optimization for support vector regression, Gaussian process, M5' model tree, multilayer perceptron neural network, reduced error pruning tree, random tree, random forest, and radial basis function neural network. The result shows that the proposed CVOA-LSTM model has high forecasting capability ($R^2 = 0.874$, root mean square error = 0.34, mean absolute error = 0.23) and outperforms the benchmarks. We conclude that CVOA-LSTM is a new tool that can be considered to forecast the hydropower dam's deformations.

1 | INTRODUCTION

Dam safety has a large effect on many aspects of life, such as life safety, property, and the dam's ecological environment; therefore, safety monitoring is an essential part of the dam management system (Salazar et al., 2017; Tu et al., 2013; R. T. Wu et al., 2019).

The primary purpose of safety monitoring is to detect abnormal movements on the surface or inside the dam to take appropriate and timely remedies. Because of the nonlinear and complex characteristics of dam movement, it is

still challenging for the managers to forecast this displacement process with high accuracy (De Sortis & Paoliani, 2007; Mata, 2011; Salazar et al., 2015).

Forecasting and diagnosing deformations of hydropower dam based on time series monitoring data play an essential role in dam safety assessment and risk management, especially with hydropower dams constructed more than 40 years ago, where the technology and computational tool used were limited (Hariri-Ardebili & Salazar, 2020). In this regard, the forecasting accuracy of deformations is highly necessary for issuing crucial decisions.

During the last 5 years, long short-term memory (LSTM) has received significant attention in time-series forecasting and analysis due to its outstanding performance in various domains (Du et al., 2020; Y. Li et al., 2020). However, designing LSTM for the deformation forecasting of hydropower dam is still challenging because it requires adapting and optimizing various parameters. Herein, we formulate the deformation forecasting as a multivariate time-series regression. The inputs are factors related to the upstream water level (UpL), the downstream water level, the air temperature, and the dam's age; the output is the horizontal deformation (HD).

Nevertheless, designing accurate LSTM models is a difficult task because the performance of LSTM is very sensitive with the hidden layer amount and the parameters employed, and they should be determined objectively. Additionally, LSTM has two major drawbacks: First, the execution time is very high, and second, the model is quite sensitive to its hyperparameters adjustment.

For these reasons, it is of utmost relevance to be able to train the deep learning models with the optimal values for the hyperparameters. This is typically done by means of optimization methods or metaheuristics, highlighting those based on bioinspired phenomena (Alba et al., 2013). This hybridization usually leads to optimized deep learning models with high performance, which is a very hot topic in the literature nowadays.

In this research, we partly fill this gap by proposing a new approach for forecasting the deformation of hydropower dam using deep learning LSTM (Lara-Benítez et al., 2020; Torres et al., 2021) optimized by the coronavirus optimization algorithm (CVOA) and named as CVOA-LSTM. The CVOA is a new optimization introduced by Martínez-Álvarez et al. (2020) that mimics the development and spread of the Severe Acute Respiratory Syndrome Coronavirus-2 (SARS-CoV-2), responsible for the coronavirus disease 2019 (COVID-19). The purpose of the CVOA here is to search and optimize the LSTM, aiming to forecast the deformation with high accuracy.

The effectiveness of the proposed LSTM-CVOA hybrid model has been used for forecasting the deformation monitoring data at the Hoa Binh hydropower dam of Vietnam, the second-largest dam in Southeast Asia. LSTM-CVOA is compared with benchmark algorithms, that is, support vector regression optimized by the sequential minimal optimization (SMO-SVR), Gaussian process (GP), M5 model tree (M5'), multi-layer neural network (MLPNeuralNet), reduced error pruning decision tree (REPTree), random tree (RT), random forest (RF), and radial basis function neural network (RBFNeuralNet). The popular hydrostatic-season-time (HST) model for dam monitoring has also been used as a baseline. Furthermore, different CVOA is compared to different optimization strategies

such as grid search (GS), random search (RS), and genetic algorithms, showing better performance for all the compared cases.

The rest of the paper is structured as follows. Section 2 discusses related works. The underlying foundations of the methods used are introduced in Section 3. Section 4 presents the case study. Section 5 details how the proposed methodology has been applied to the case-study data. Section 6 reports the results achieved and discusses them. Finally, conclusions, limitations, and future works are summarized in Section 7.

2 | RELATED WORKS

Various methods have been proposed for forecasting and analyzing the dam displacement, and they could be categorized as deterministic group, statistical group, and machine learning methods (Salazar et al., 2017). Based on the definition, the deterministic group refers to the physical models, but physical models do not necessarily need to be deterministic. In fact, they can be used as a simulation tool in a probabilistic assessment. For example, the input uncertainties can be quantified, sampled, and propagated through the simulation model to generate probabilistic outputs. In addition, one could also conduct simulation optimization.

Deterministic methods are well-known as the finite element method (Gurbuz, 2011; Pereira et al., 2020), boundary element method (Antes & Von Estorff, 1987). In these methods, parameters/quantities related to structures, such as material, stress-strain, seepage, are employed to establish mathematical functions to relate the dam's displacement over time. Therefore, they are commonly used in the dam displacement analysis at the constructing and first filling phases.

When the monitoring time-series data is long enough, statistical methods, that is, hydrostatic-seasonal-time (Sigtryggisdóttir et al., 2018), have more advantages than deterministic methods in terms of more straightforward function form and calculating speed (Shao et al., 2017; Stojanovic et al., 2013; Wei et al., 2020). However, in some cases, it is impossible to obtain enough time-series data, so the reliability of the methods is not guaranteed. Besides, as we know, dam deformation is a typical nonlinear process, so it is difficult for statistical methods to forecast with high accuracy (Salazar et al., 2015).

Recently, machine learning, that is, neural networks (Kao & Loh, 2013; Mata, 2011; Ranković et al., 2012; Rodríguez et al., 2019; Salazar et al., 2017), artificial immune algorithm (Xi et al., 2011), support vector machine (SVM; Ranković et al., 2014; Salazar et al., 2015; Su et al., 2017; Tabari & Sanayei, 2018; Wei et al., 2020; Zheng



et al., 2013), wavelet SVM (Su et al., 2018), RF and boosted regression tree (Salazar et al., 2016), GP (Kang & Li, 2020), multivariate adaptive regression splines (Salazar et al., 2015), adaptive neural fuzzy inference system (Bui et al., 2018; Ranković et al., 2012; Taormina & Chau, 2015), multi-block-based diagnosis method (Qin et al., 2017), and signal-residual amendment (Wei et al., 2020), have successfully forecasted dam displacement with great accuracy results.

More recently, recurrent neural networks (RNN) and variants like LSTM networks, introduced by Hochreiter and Schmidhuber (1997), have received great attention in solving regression problems in various engineering fields (Chen et al., 2020; Hua et al., 2019; Ni et al., 2020; Ni et al., 2020; Divina et al., 2020; Torres et al., 2018; Torres, Troncoso, et al., 2019; Zhang et al., 2019). Moreover, much attention has been paid to the optimization of such models, which are quite sensitive to the parameters setting (Charte et al., 2020; Siqueira et al., 2020; Thurnhofer-Hemsi et al., 2020). Ribeiro et al. (2019) compared Seasonal Autoregressive Integrated Moving Average (SARIMA), Seasonal Autoregressive Integrated Moving Average Exogenous model (SARIMAX), and a hybrid SARIMAX-LSTM for forecasting the concrete dam's displacements with a report that the hybrid model is capable of providing a better forecast accuracy. Yang et al. (2020) employed LSTM to predict a concrete dam's deformation with good results (Rafiei et al., 2017; Rafiei and Adeli, 2017). Y. Li et al. (2020) proposed an ensemble of the Loess-based seasonal-trend decomposition, extra trees, and LSTM for analyzing the displacements of a concrete dam with outstanding forecasting performance. Liu et al. (2020) consider the integration of the moving average technique, principal component analysis, and LSTM for predicting displacements of arch dams with a conclusion that the LSTM-MA delivers better prediction results.

Overall, though these machine learning algorithms require long time-series data, they are potent tools in nonlinear process relationships of the dam displacement and influence of external factors. Nevertheless, there is no consensus on which machine algorithm is the best for forecasting deformations of dams. As a result, the exploration and development of new algorithms to improve forecasting capability is still an essential issue in dam deformation analysis.

3 | CASE STUDY

3.1 | Overview of the hydropower dam

In this research, a hydropower dam located in the Da river section flowing through the Hoa Binh city in northwest Vietnam was adopted as a case study (see Figure 1).

This is the second largest hydroelectric project in Southeast Asia after the Son La hydropower plant in the north of Vietnam that was completed in 2012. The hydropower project, which was designed, supplied equipment, and constructed by the former Soviet Union started on November 6, 1979, and was completed on December 20, 1994 (Vladimirov et al., 2003).

The project consists of eight hydroelectric generators with a total capacity of 1920 MW, and they were located in the underground of an effusive rock hill, which can suffer from seismic and earthquakes up to Level 8 (Ezersky & Eppelbaum, 2017; Ezerskii et al., 1990). In the first period of the operation, the electricity production accounted for about 40% of the total production in Vietnam, and during the last 26 years, this project has produced about 230 billion kWh. Besides the power supply, the project's other primary function is to regulate and control floods to ensure safety for both the Hanoi capital and the Red River Delta provinces, where the total population is more than 22.5 million people in 2019 (GSO, 2020).

This project's dam was constructed from 1981 to 1990, and this is the clay core-based rock-earth fill dam with a length and height of 734 and 128 m, respectively. The highest water level is designed at 120 m, whereas the lowest level is 80 m. The dam can withstand the highest difference in height between the upstream and the downstream water levels of 102 m.

The monitoring data at the dam showed that the difference in the water flow between the dry and flood seasons is large. For example, in 1971, a recorded flow in the dry season is 600 m³/s, and the flood season is up to 14800 m³/s. It should be noted that the total reservoir area is around 208 km², and the total water storage volume is 9.45 billion m³.

3.2 | Health monitoring data

To monitor the dam behavior, a geodetic network with 12 points has been established on the downstream face, in which 6 points (PV2, PV4, PV6, PV8, PV10, PV12) have been placed at 123 m high, whereas the six remaining points (PV1, PV3, PV5, PV7, PV9, PV11) have setup at 75 m high. The horizontal movement of those points was measured and determined using a triangular geodetic network measured. Therein, theodolites were used for the measurement before the year 2000, and then, total stations have been replaced and used for the measurement until now.

In this analysis, the HD data measured at the PV6 point in around 22 years, from January 23, 1998, to September 5, 2019, were considered. The PV6 point was selected because it is located near the middle of the dam (123 m high).



FIGURE 1 Hoa Binh hydropower dam: (a) Location of the dam; (b) the dam view from the google earth; (c) the dam from the downstream view; and (d) the dam from the upstream view (photo courtesy of Ngoc Thanh)

TABLE 1 A statistical overview of the time-series data for the horizontal deformation (HD) analysis in this research

No.	Variable	Unit	Min	Max	Mean	Std. error	Std. dev
1	HD	m	0.088	0.199	0.121	0.001	0.022
2	Upstream water level	m	78.56	117.25	104.92	0.64	10.38
3	Downstream water level	m	9.65	21.65	13.53	0.13	2.16
4	Air temperature	Degree	12.40	32.30	24.37	0.29	4.72
5	Dam age	Month	92.47	355.63	222.45	4.77	76.95

Together with the HD data, other related time-series data were monitored, including UpL, downstream water level (DoL), air temperature (t), and the dam age in month (θ) were also considered. The statistical description of the monitoring data used in this analysis is shown in Table 1 and graphical presentations of these data are shown in Figure 2.

According to the report of Hoa Binh hydropower company, from the year 2005, TCA2003 of Leica (precision

of 0.5" for horizontal displacement angular and 1 mm + 1 ppm/0.3 s for distance) was used to measure the 31 angles and 28 distances in the monitoring network.

After adjusting the computation of each monitoring epoch, the coordinates and position of all monitoring points are determined inaccuracy of 1 mm or below. Thus, this value also is the accuracy of individual value in each monitoring epoch and is chosen as the standard error of dam horizontal displacement time-series in Table 1.

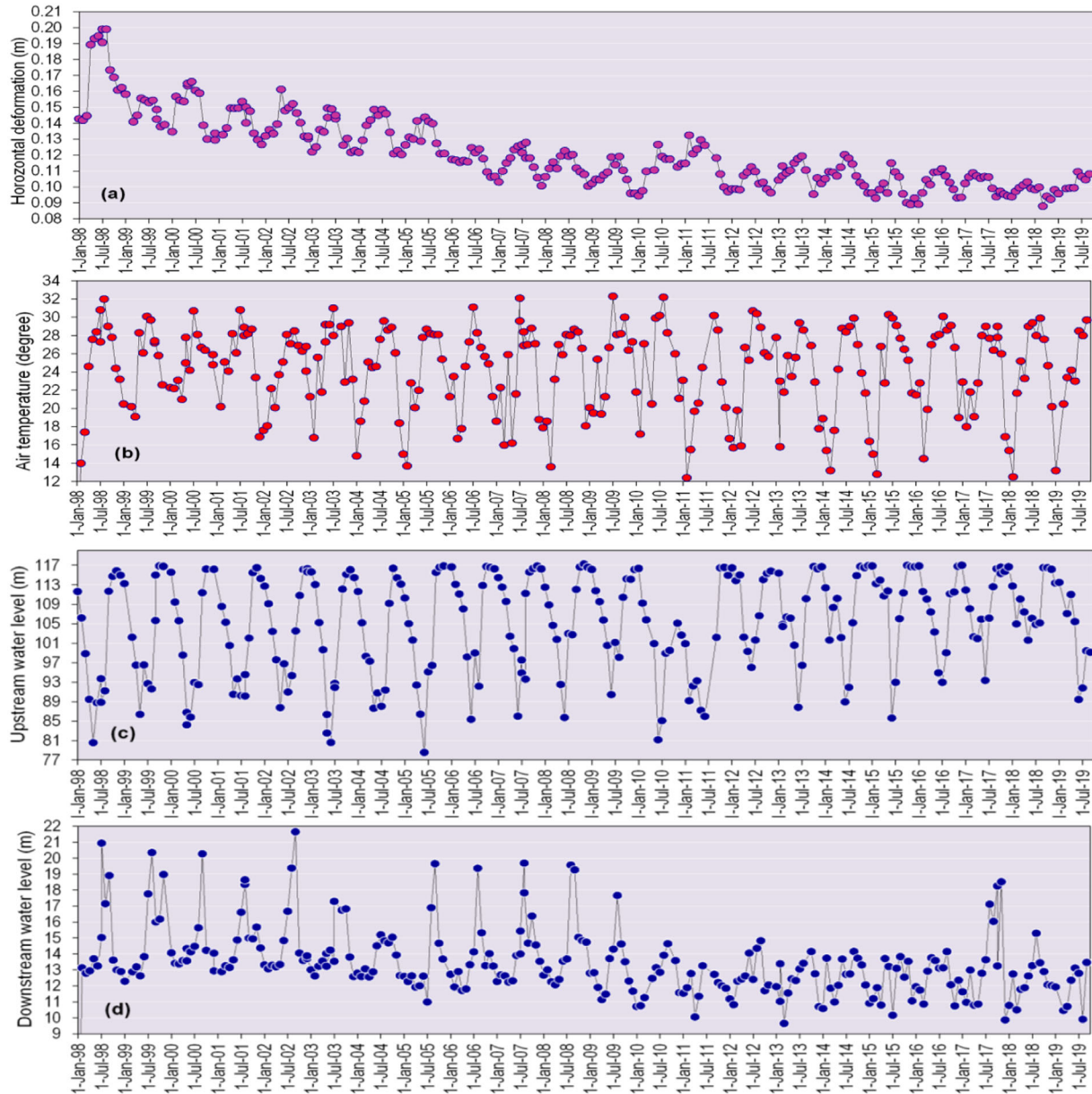


FIGURE 2 Time series monitoring data: (a) horizontal deformation (HD; m) at the PV6 station and (b) air temperature ($^{\circ}$)

4 | BACKGROUND OF THE EMPLOYED ALGORITHM

This section provides the necessary theoretical information for a better understanding of the proposed approach. Thus, Section 4.1 introduces the LSTM network and Section 4.2, the CVOA, used to optimize the deep learning model hyperparameters.

4.1 | LSTM networks

This section describes the mathematical foundations underlying the LSTM network. LSTMs are RNN architectures used in deep learning. Such architecture is particularly suitable to process images, video, or speech, leading to successful applications in civil and infrastructure engineering (Jeong et al., 2020; Jiang & Zhang, 2020; F. Ni et al.,

2019; Xu et al., 2020). However, it can also be applied to the field of time-series forecasting, as widely discussed in the literature, given their ability to deal with lags of arbitrary duration.

Standard RNNs suffer from gradient issues, which consists of decreasing the gradient as the number of layers increases. Actually, for RNNs with a high number of layers, the gradient becomes almost null, preventing the network from learning. For this reason, these networks have a short-term memory and do not obtain good results when dealing with long sequences that require memorizing all the information contained in the complete sequence.

LSTM recurrent networks have emerged to solve the vanishing gradient problem (Hochreiter et al., 1997), using three gates to keep longstanding relevant information and discard irrelevant information. These gates are:

1. Forget gate, Γ^f . It decides the information that should be discarded or saved. A value near to 0 means that the past information is forgotten, while a value near 1 means that it is kept.
2. Update gate, Γ^u . It decides which new information c_t to use to update the c_t memory state. Thus, c_t is updated using both Γ^f and Γ^u .
3. Output gate, Γ^o . It decides which is the output value that will be the input of the next hidden unit.

The information of the a_{t-1} previous hidden unit and the information of the x_t current input is passed through the sigmoid activation function, σ , to compute all the gate values and through the tanh activation function to compute the c_t new information, which will be used to update the values. The equations defining an LTSM unit are:

$$c_t = \tanh(W_c [a_{t-1}, x_t] + b_c) \tag{1}$$

$$\Gamma^u = \sigma(W_u [a_{t-1}, x_t] + b_u) \tag{2}$$

$$\Gamma^f = \sigma(W_f [a_{t-1}, x_t] + b_f) \tag{3}$$

$$\Gamma^o = \sigma(W_o [a_{t-1}, x_t] + b_o) \tag{4}$$

$$c_t = \Gamma^{u*} c_t + \Gamma^{f*} c_{t-1} \tag{5}$$

$$a_t = \Gamma^{o*} \tanh(c_t) \tag{6}$$

where $W_u, W_f, W_o, b_u, b_f,$ and b_o are the weights and the bias that govern the behavior of the Γ^u, Γ^f and Γ^o gates, respectively, whereas W_c and b_c are the weights and bias of the c_t memory cell candidate.

An illustration of a hidden unit in an LSTM deep learning model is shown in Figure 3.

4.2 | CVOA

The CVOA is a bioinspired metaheuristic first proposed by Martínez-Álvarez et al. (2020). CVOA was developed based on the COVID-19 spreading model, the disease caused by the SARS-CoV-2 virus, first reported in 2019. One of the main features lies in its remarkable trade-off between intensification and diversification to efficiently explore the search space. In this work, the CVOA is employed to optimize the hyperparameters of an LSTM model, but the authors claimed that it can be used to optimize any kind of algorithm. The LSTM hybridization was done through a new dynamic individual codification proposal. Every individual can be of different lengths, according to the number of layers the individual codifies. Furthermore, real data from the Spanish electricity market were used to assess its performance, reaching quite remarkable results in terms of accuracy and outperforming other well-established models optimized with other metaheuristics.

CVOA mimics how the coronavirus infects and spreads the disease. In particular, every infected individual identifies one solution, and the infection process stands for the exploration of new solutions. As for any metaheuristic, CVOA must ensure both intensification and diversification.

On the one hand, the intensification is controlled as follows. It is well-known that the infection rate for COVID-19 is 3 when no face masks are worn, social distancing T is not followed, or no vaccines had been inoculated into the population (WHO, 2021), which means that every infected individual can infect three more individuals on average. In other words, given a solution (infected individual), three new solutions are explored (three new individuals are infected from the current one). Additionally, the existence of super-spreaders has also been reported in the literature. This involves a high infection rate for such individuals; that is, certain infected individuals will infect more than three individuals, on average.

On the other hand, the diversification is controlled by considering that some individuals can travel and visit regions of the search space that are far away. In other words, travelers will lead to the exploration of new solutions quite dissimilar.

It is worth mentioning that all probabilities and rates have been retrieved from the real values of the COVID-19. This prevents the user from consuming time in adjusting the CVOA parameters because all of them are set by default. However, different values can be assigned to

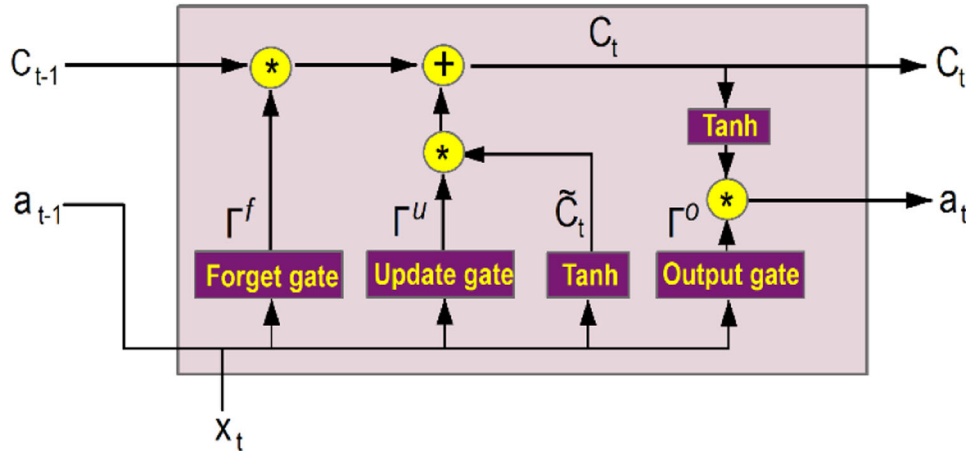


FIGURE 3 Description of the hidden unit in a long short-term memory (LSTM), * and + operators identify the multiplication and sum of the element-wise vector, respectively

simulate different strains, with higher fatality rates or higher infection rates, for instance. A very useful feature is the parallel implementation, also proposed in this work, since it explains how to run different strains with different setup values.

The main CVOA steps can be summarized as follows:

1. Step 1: Patient-zero (PZ) generation. This step consists of randomly generating the initial solution. If previous knowledge about the problem is known, this step can be avoided and the optimization process can be started from any arbitrary solution.
2. Step 2: Spreading the disease. Every solution will infect new ones, according to some parameters such as the probability of death (solutions that will not be explored), spreading rate (the number of new solutions explored from a previous one), super-spreading rate (same as the spreading rate but with higher values), traveling probability (infection of quite dissimilar solutions for a better exploration of the search space).
3. Step 3: Updating populations. CVOA maintains three different sets of solutions: infected (current iteration), deaths (solutions that cannot infect anymore), and recovered (solutions already explored that might re-infect if the re-infection probability is met).
4. Step 4: Stop criterion. CVOA ends its execution after a given number of iterations or if the infected population is empty.

5 | PROPOSED HYBRID APPROACH FOR DEFORMATION FORECASTING OF HYDROPOWER DAMS

This section describes the dataset (Section 5.1) and discusses the configuration for the CVOA-LSTM (Section 5.2).

5.1 | Dataset description

As mentioned above, in this work, we employed the measured data at the PV6 point (see Figure 1) for nearly 22 years, from January 23, 1998, to September 5, 2019, with 260 measured cycles, retrieved on a monthly basis. Since machine learning models are based on time-series measured data only, without considering the physical characteristics of the dam materials in the modeling (Salazar et al., 2016), therefore, to forecast the dam deformation, it is necessary to determine its influencing factors.

Literature review shows that hydraulic load, temperature, and dam age (Bui et al., 2018; Dai et al., 2018; Kang et al., 2017; Lin et al., 2019; Luo et al., 2019; Ren et al., 2020; Shi et al., 2018; Zou et al., 2018) are the main influencing factors; therefore, in this research, UpL , UpL , t , and θ were considered.

Because the dam deformation modeling in this research uses the concept the HST that is widely accepted and used by engineers in the dam modeling (Salazar et al., 2015), therefore, higher orders of UpL should be considered, that is, UpL^2 , UpL^3 , UpL^4 , whereas time lags of t can be used as t_{15} , t_{30} , t_{45} , and t_{60} , which are the air temperature at 15, 30, 45, and 60 days, respectively, before each measuring cycle.

Regarding the dam age, both θ and $\ln(\theta)$ should be used (Stojanovic et al., 2013). As a result, 12 input factors used are UpL , UpL^2 , UpL^3 , UpL^4 , DoL , t , t_{15} , t_{30} , t_{45} , t_{60} , θ , $\ln(\theta)$, whereas the output is the HD value. In order to avoid a potential bias deformation modeling of the dam, all input values were normalized in a range from 0 to 1 (Bui et al., 2018).

Training the model is a key step in time-series forecasting. The use of k -fold cross-validation is not considered in this work due to some well-known limitations in time-series forecasting: use of future values to predict past ones,



the existence of gaps in time leading to the loss of relevant information, and data leakage in training and test. However, the time-series data were separated into two subsets, with a 70/30 ratio. The first subset is that the training dataset has 160 cycles, measured from January 23, 1998, to February 17, 2011 (with, again, a 70/30 ratio for training and validation), whereas the second subset is the test set consisting of 100 measured cycles from March 14, 2011, to September 5, 2019. Other similar strategies such as time-series split and block time-series split () could have been used, but preliminary results generated worse results, probably due to the small size of the dataset.

Besides, it was expected that data de-trending and scaling may have improved the results, but, unfortunately, such preliminary experimentation led to worse results in terms of accuracy and all performance metrics considered in this work.

5.2 | Configuring the CVOA-LSTM model

For establishing the LSTM model for forecasting the deformation of the hydropower dam, it is necessary to properly determine three parameters: number of layers (L), learning rate (LR), and dropout (Drop), because they strongly influence the forecasting capability of the resulting model. The literature review showed that no thumb rule is available for the determination of these parameters; therefore, in this work, the CVOA is proposed to search and optimize the three elements:

1. Number of hidden layers (L): This element identifies the possible number of layers in the architecture of the LSTM. In this work, a restriction to $1 < L \leq 11$ was considered.
2. Learning rate (LR): This variable encodes the learning rate used in the LSTM. In this research, we considered values as 10^0 , 10^{-1} , 10^{-2} , 10^{-3} , 10^{-4} , and 10^{-5} .
3. Dropout (Drop): This parameter encodes the LSTM dropout in the interval $[0, 0.45]$, with step 0.05.

Herein, a three-dimensional searching space (L, LR, and Drop) is established. L is of the utmost relevance and is highly related to the variable length of the individual because, for every layer, the number of neurons must be encoded. For instance, if $L = 4$, then four new values would be optimized, corresponding to the number of neurons existing in each of these four layers. The number of possible neurons per layer is in the range $[25, 300]$, with step 25.

An illustration of the individual codification proposed to hybridize the CVOA-LSTM model is depicted in Figure 4. The parameters adopted for the CVOA in this analysis are depicted in Table 2. It is worth mentioning that

one of the main features of CVOA is that such configuration is suggested to be always the same (Martínez-Álvarez et al., 2020) since CVOA mimics the COVID-19 spreading model, and the metrics and statistics are well-known. It is also true that these metrics have evolved over time as the pandemic has shown new statistics across the world. But it has been decided to use the original parameter values proposed since the use of some others may deeply vary the functioning of CVOA, which is not the scope of this paper.

6 | RESULTS AND ANALYSIS

Please note that, in this project, the time-series data were processed and visualized using Microsoft Excel 2020 and ArcGIS Pro 2.6. The code of the proposed hybrid model is available at Martínez-Álvarez et al. (2020), whereas the benchmark algorithms above are available at WEKA 3.7.10.

6.1 | Objective function and performance assessment of the CVOA-LSTM model

In order to measure if the combination of the three parameters (L, LR, and Drop) is the best or not, a cost function must be employed. In this research, mean absolute error (MAE) in Equation (7) was employed as the cost function:

$$\text{MAE} = \frac{1}{n} \sum_{i=1}^n |d_i - \hat{d}_i| \quad (7)$$

The selection of this metric lies in the need of discovering absolute values for the dam displacements. While other problems are likely to express the errors in relative terms and use metrics such as mean absolute percentage error, in this study, this value does not provide relevant information.

Besides, the quality of the resulting model was further assessed and quantified using the popular statistical metrics in the field of HD, such as root mean square error (RMSE) and coefficient of determination (R^2 ; M. Li et al., 2019; Salazar et al., 2017; Su et al., 2018), as shown below:

$$\text{RMSE} = \sqrt{\frac{1}{n} \sum_{i=1}^n (d_i - \hat{d}_i)^2} \quad (8)$$

$$R^2 = 1 - \frac{\sum_{i=1}^n (d_i - \hat{d}_i)^2}{\sum_{i=1}^n (d_i - \bar{d}_i)^2} \quad (9)$$

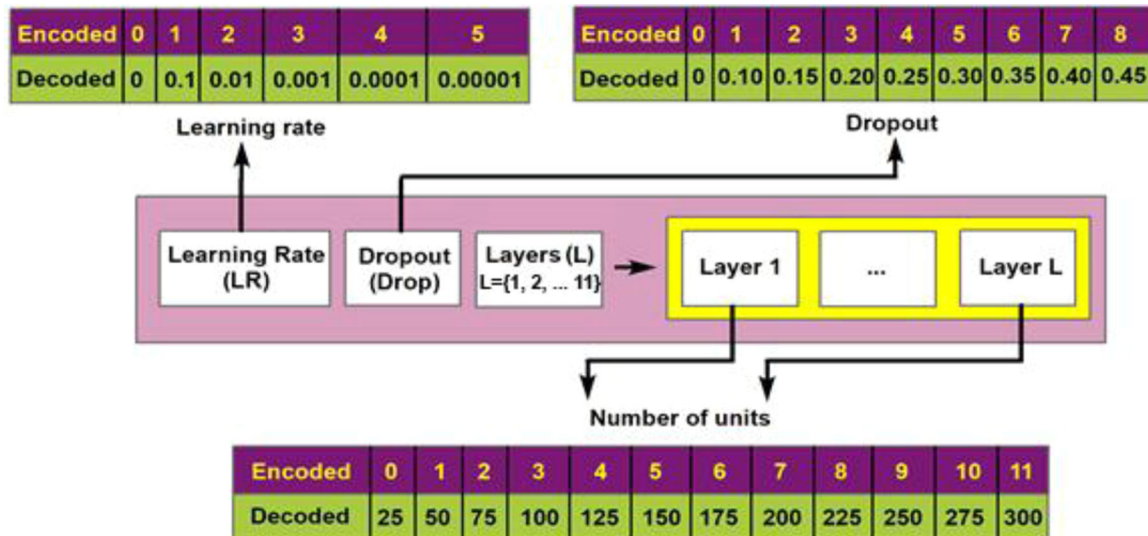


FIGURE 4 Proposed codification for the individual in this research

TABLE 2 The employed parameters for the coronavirus optimization algorithm (CVOA) algorithm

No	Parameter	Description	Value
1	Prob. D	Probability of dying	0.05
2	Prob. SS	Probability of being a super-spreader	0.10
3	Prob. RI.	Probability of reinfection	0.02
4	Prob. IS.	Probability for an individual of being isolated	0.70
5	Prob. TV	Probability of traveling to other search space regions	0.10
6	Social Dist.	Number of iterations without social distancing	[7, 12]
7	Pan. DR.	Number iterations	20
8	Strains	Number of threads	4
9	Np	Number of coronavirus in the population	30

6.2 | Training and validating results of the CVOA-LSTM model

The training process for the CVOA-LSTM was started by randomly generating an initial individual and named as PZ. Herein, the position of PZ with three coordinates (L, LR, and Drop) in the three-dimensional searching space is a solution for the CVOA-LSTM, and the quality of the solution is measured by MAE. The training process was continued where the spreading the disease phase was activated, and 30 individuals were affected. Then, every individual infects new ones, and a new population was updated. With the new population, the MAE value for each CVOA-LSTM model corresponding to each individual was computed and compared to find the optimized one. This was an iteration process. The proposed CVOA-LSTM approach has obtained very competitive results, with RMSE = 0.26 cm, MAE = 0.23 cm, and $R^2 = 0.912$, which were reached after the ninth iteration and just some improvements were

reported during the next five iterations. Then, no improvement was derived. For this reason, the stop criterion was met, and the execution was stopped after only 12 iterations.

Table 3 shows the metrics evolve after each iteration. We see that the best results are derived with the individual [4, 3, 2] + [3, 3], which were decoded to the following values: the learning rate is 10^{-4} , the dropout is 0.2, and the number of the hidden layers is 2, whereas the number of neurons for each layer is 100.

After the 12 training iterations, RMSE and MAE of the CVOA-LSTM model are 0.24 and 0.21 cm, respectively, which are significantly lower than the standard deviation value of the HD (2.20 cm, Table 1). These indicate that the CVOA-LSTM model performed well. R^2 is 0.988 (Figure 5a), denoting a small difference between the measured and the computed values. The difference of RMSE and MAE values of the CVOA-LSTM model is 0.03 cm indicating that the variance of the error in the training dataset is low (Figure 5a).

TABLE 3 Performance of the CVOA-LSTM model for the HD in this analysis

Iteration	Root mean square error (RMSE; cm)	Mean absolute error (MAE; cm)	R ²
1	10.15	10.13	0.372
2	3.15	3.05	0.526
3	0.74	0.62	0.684
4	0.41	0.32	0.728
5	0.38	0.31	0.790
6	0.37	0.30	0.812
7	0.34	0.29	0.852
8	0.31	0.26	0.886
9	0.26	0.23	0.912
10	0.24	0.21	0.988
11	0.24	0.21	0.988
12	0.24	0.21	0.988

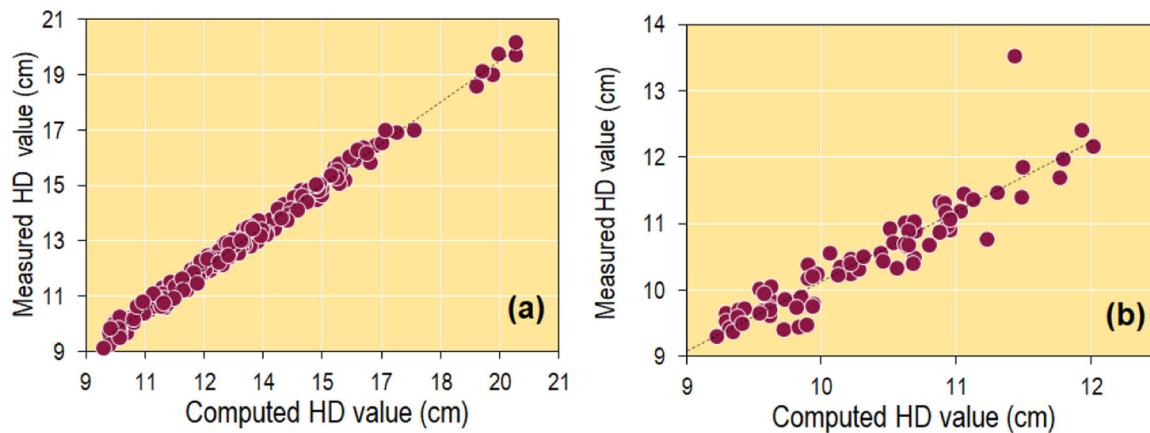


FIGURE 5 R² of the CVOA-LSTM model: (a) the validation set and (b) the test set

The running time for these experiments during the training phase was 10,162 s.

The forecasting capability of the HD of the CVOA-LSTM model is assessed using the 100 samples measured from March 14, 2011, to September 5, 2019, in the validating dataset. The result is shown in Figures 5b and 6 and Table 4. RMSE, MAE, and R² of the CVOA-LSTM model are 0.34 cm, 0.23 cm, and 0.874, respectively, denoting that the proposed model performs forecasting well. The small difference (0.11 cm) between the RMSE value and the MAE value indicates a low variance of the error in forecasting the HD.

6.3 | Comparison with other machine learning regressions for the HD

The validity of the CVOA-LSTM model for forecasting the HD of hydropower dam was assessed by compar-

ing its performance with nine well-established state-of-the-art machine learning regression algorithms, that is, SMO-SVR, GP, M5', MLPNeuralNet, REPTree, RT, RF, and RBFNeuralNet. Furthermore, HST has been used given its popularity for dam deformation forecasting. Finally, other optimizing strategies such as GS, RS, and genetic algorithms have been used to find the LSTM hyperparameters. The selection of them is an attempt of covering different learning paradigms and provide comparisons as robust as possible.

For the SMO-SVR model, the radial basis function (RBF) was used, and the two turning parameters of the model, the regularization (*C*) and the kernel width (γ), were determined using the popular grid-search algorithm. As a result, *C* = 5.5 and γ = 0.0062 were found the best for this hydropower dam data.

For the GP model, the kernel of RBF was employed. Herein, the two parameters, the level of Gaussian noise (*g*) and the kernel width (γ), were also searched and

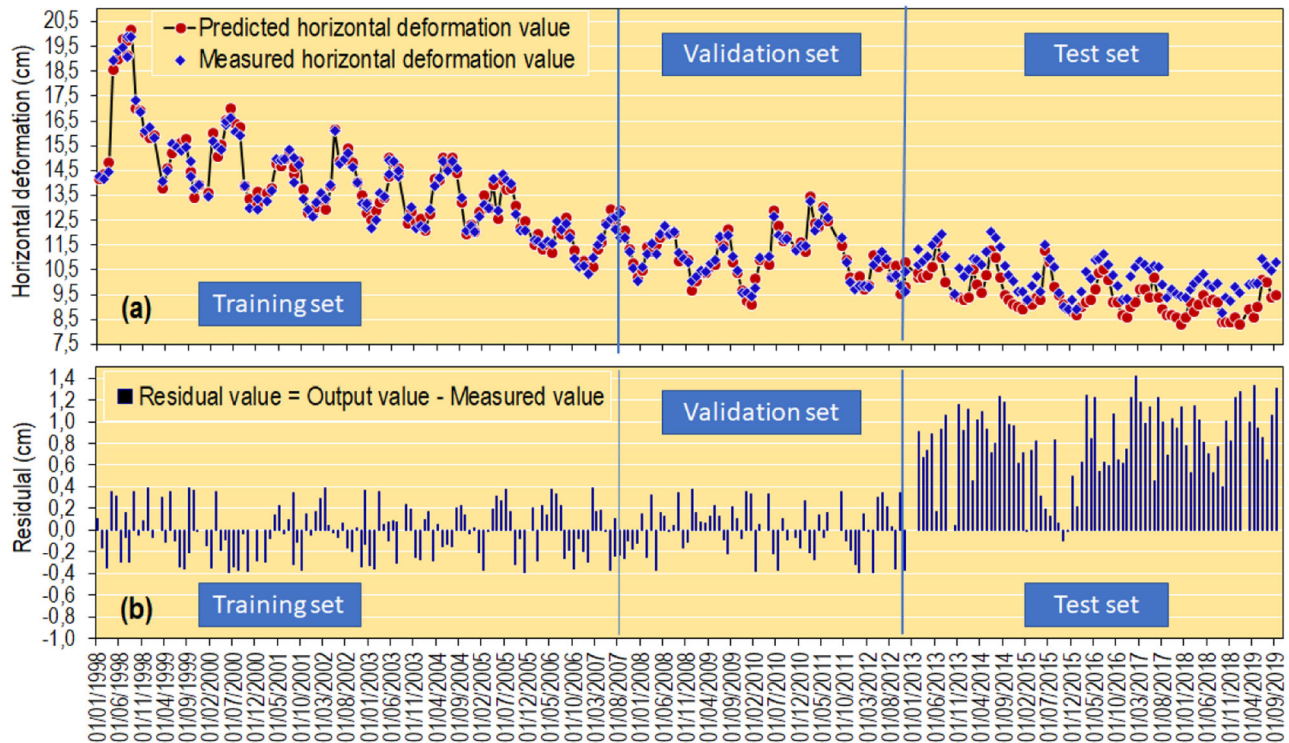


FIGURE 6 Performance of the CVOA-LSTM model: (a) Predicted HD values versus measured HD value and (b) residual values

TABLE 4 Performance of the nine state-of-the-art machine learning regression models for forecasting the hydropower dam deformation

HD model	Validation set			Test set		
	RMSE (cm)	MAE (cm)	R ²	RMSE (cm)	MAE (cm)	R ²
SMO-SVR	0.75	0.53	0.884	0.87	0.80	0.792
Gaussian process (GP)	0.90	0.63	0.865	0.47	0.41	0.764
M5 model tree (M5')	0.61	0.47	0.922	0.71	0.63	0.781
MLPNeuralNet	0.75	0.57	0.882	1.06	0.99	0.759
REPTree	0.66	0.48	0.903	0.93	0.79	0.436
Random tree (RT)	0.03	0.02	0.998	0.56	0.48	0.449
Random forest (RF)	0.23	0.18	0.990	0.81	0.68	0.496
RBFNeuralNet	1.19	0.93	0.701	1.33	1.20	0.446
HST	0.78	0.58	0.901	0.85	0.67	0.812
GS-LSTM	0.65	0.49	0.943	0.85	0.69	0.833
RS-LSTM	0.61	0.43	0.956	0.82	0.59	0.821
GA-LSTM	0.65	0.46	0.932	0.78	0.56	0.847
CVOA-LSTM	0.24	0.21	0.988	0.34	0.23	0.874

Abbreviations: GS-LSTM, grid search-LSTM; HST, hydrostatic-season-time; MLPNeuralNet, multilayer perceptron neural network; RBFNeuralNet, radial basis function neural network; REPTree, reduced error pruning tree; RS-LSTM, random search-LSTM; SMO-SVR, sequential minimal optimization for support vector regression.

optimized using the aforementioned grid-search algorithm. The result showed that $g = 0.95$ and $\gamma = 0.004$ are the optimized values for this analysis.

For the M5', the minimum number of instances at a leaf node of 1 was used.

Regarding the MLPNeuralNet model, the structure with two neurons in the hidden layer showed the best result. We used a learning rate (η) of 0.3 and a momentum (α) of 0.2. Besides, the logistic sigmoid and linear were used as the activation and transfer functions, respectively.



TABLE 5 Wilcoxon rank-sum results for all the evaluated methods

Models	GP	M5'	MLP	REPTree	RT	RF	RBF	HST	GS-LSTM	RS-LSTM	GA-LSTM	CVOA-LSTM
SMO-SVR	**	**	*	**	*	**	**	*	**	**	**	**
GP		**	**	**	**	**	**	**	**	**	**	**
M5'			**	*	*	**	**	*	**	**	**	**
MLP				**	*	**	*	**	**	**	**	**
REPTree					*	*	**	**	**	**	**	**
RT						**	*	**	**	**	**	**
RF							**	**	**	**	**	**
RBF								**	**	**	**	**
HST									**	**	**	**
GS-LSTM										*	**	**
RS-LSTM											*	*
GA-LSTM												**

Abbreviations: GS-LSTM, grid search-LSTM; HST, hydrostatic-season-time; MLPNeuralNet, multilayer perceptron neural network; RBFNeuralNet, radial basis function neural network; REPTree, reduced error pruning tree; RS-LSTM, random search-LSTM; SMO-SVR, sequential minimal optimization for support vector regression.

** and * denote $p < 0.001$ and $p < 0.05$, respectively.

For the REPTree model and RT model, the minimum total weight of the samples in a leaf used is 2.0. Regarding the RF model, 500 trees were used to ensure the diversity of the ensemble forest (Alam et al., 2020). With reference to the RBFNeuralNet model, nine clusters were adopted using a trial and test analysis. The performance of these machine learning regression models for forecasting the hydropower dam deformation is shown in Table 4 and Figures A1 and A2.

As for the HST model, it is composed of functions multiplied by coefficients estimated using the multiple linear regression method. Such coefficients model the elastic effect hydrostatic pressure, the thermal component, and the irreversible displacements (Belmokre et al., 2021; Sigtryggisdóttir et al., 2018).

Finally, three different metaheuristics have been used to optimize the LSTM network, in particular the GS strategy proposed in Torres et al. (2019), the RS proposed in Torres et al. (2018), and the genetic algorithm proposed in Divina et al. (2020). Note that all of them were designed and developed to optimize LSTM networks.

Regarding the nine well-established machine learning methods, we observe that, excepting the RBFNeuralNet model, the other models fit well with the training dataset (Table 4). The highest degree of fit is the RT model ($R^2 = 0.998$, RMSE = 0.03, MAE = 0.02), which is perhaps due to overfitting. The RF model is the second-best model but, this time, its values do not seem to exhibit overfitting. ($R^2 = 0.990$, RMSE = 0.23, MAE = 0.18). They are followed by the M5' model ($R^2 = 0.922$, RMSE = 0.61, MAE = 0.47), the REPTree model ($R^2 = 0.903$, RMSE = 0.66, MAE = 0.48), the SMO-SVR model ($R^2 = 0.884$, RMSE = 0.75, MAE = 0.53), MLP-

NeuralNet model ($R^2 = 0.882$, RMSE = 0.75, MAE = 0.57), the GP model ($R^2 = 0.865$, RMSE = 0.90, MAE = 0.63), and the RBFNeuralNet model ($R^2 = 0.701$, RMSE = 1.19, MAE = 0.93). Compared to the CVOA-LSTM model ($R^2 = 0.988$, RMSE = 0.24, MAE = 0.21), the RT model and the RF model perform slightly better, whereas the other benchmark models have a lower degree of fit with the training dataset (Table 4 and Figures A1 and A2).

It is worth noting that HST has a remarkable performance in the training set even though is far from being the best result ($R^2 = 0.901$, RMSE = 0.78, MAE = 0.58).

The three other optimization methods reach similar results, being slightly better than HST (GS-LSTM: $R^2 = 0.943$, RMSE = 0.65, MAE = 0.49; RS-LSTM: $R^2 = 0.956$, RMSE = 0.61, MAE = 0.43; GA-LSTM: $R^2 = 0.932$, RMSE = 0.65, MAE = 0.46).

Regarding the forecasting capability of the eight state-of-the-art machine learning regression models, the validation data was used, and the result is presented in Table 4 and Figures A1–A3. It could be seen that the SMO-SVR model ($R^2 = 0.792$, RMSE = 0.87, MAE = 0.80) has the highest forecasting capability, followed by the M5' model ($R^2 = 0.781$, RMSE = 0.71, MAE = 0.63), the GP ($R^2 = 0.764$, RMSE = 0.47, MAE = 0.41), the MLPNeuralNet model ($R^2 = 0.759$, RMSE = 1.06, MAE = 0.99). The other models have poor performance, the RF model ($R^2 = 0.496$, RMSE = 0.81, MAE = 0.68), the RT model ($R^2 = 0.449$, RMSE = 0.56, MAE = 0.48), and the REPTree model ($R^2 = 0.436$, RMSE = 0.93, MAE = 0.79).

HST reaches the best results in terms of the R^2 and is outperformed by a few methods in terms of RMSE and MAE ($R^2 = 0.812$, RMSE = 0.85, MAE = 0.67). But it is



especially remarkable that training and test results do not differ much.

That is, it exhibits a robustness superior to the previous methods. GS-LSTM ($R^2 = 0.833$, RMSE = 0.85, MAE = 0.69), RS-LSTM ($R^2 = 0.821$, RMSE = 0.82, MAE = 0.59), and GA-LSTM ($R^2 = 0.847$, RMSE = 0.78, MAE = 0.56) clearly outperform the eight state-of-the-art methods in all the metrics considered. Additionally, although GS-LSTM shows similar performance to HST, RS-LSTM and GA-LSTM also outperform it, achieving very competitive results.

Nevertheless, the forecasting capabilities of the eight state-of-the-art machine learning regression models, HST and GS-LSTM, RS-LSTM and GA-LSTM are clearly lower than that of the proposed CVOA-LSTM model ($R^2 = 0.874$, RMSE = 0.34, MAE = 0.23).

Finally, the running time for the eight state-of-the-art methods was 37 s on average. As for the HST model, it took 13 s. Finally, GS-LSTM, RS-LSTM, and GA-LSTM took 7340, 4398, and 9854 s, respectively. CVOA-LSTM took 10265 s.

6.4 | Discussion of the results

The result in this study shows that the forecasting accuracy is strongly dependent on the number of L, LR, and Drop of the LSTM model; therefore, it is necessary to determine them properly. Herein, the new CVOA is proposed to search and optimize these parameters. As a result, the high forecasting performance of the hybrid CVOA-LSTM model (Table 4 and Figures 5 and 6) indicates that the CVOA algorithm works efficiently in finding optimized values for the three parameters. Thus, with only 12 iterations, 36 possible combinations of L, LR, and Drop were explored to search these optimized values, which indicate that the CVOA algorithm has a high convergence speed.

The efficacy of the CVOA-LSTM model for forecasting the deformation of hydropower dam was checked by comparing eight soft computing (C. L. Wu & Chau, 2013) algorithms, SMO-SVR, GP, and M5', MLPNeuralNet, REPTree, RT, RF, RBFNeuralNet. They are state-of-the-art algorithms that have been used for predicting dam behaviors in various studies. The outstanding forecasting performance of the CVOA-LSTM model (Table 4 and Figures 5 and 6) indicates that the proposed CVOA-LSTM is a new model that should be considered for dam safety monitoring.

Among the eight soft computing models, RF, RT, REPTree, and RBFNeuralNet show some problems of overfitting, which were revealed by high performance in the training phase but poor forecasting results. This is because the first three models use the weighted average method

to compute weights from the training data. However, due to the damage, the deformation values in the validation dataset are out of the range, compared to those of the training dataset. Consequently, these models have some problems in extrapolating deformation values far from those they have learned.

Regarding the data used in hydropower dam deformation forecasting, it is suggested that the monitoring data for training and validating should be at least 5 and 3 years, respectively (ICLA, 2012), to ensure reasonable accuracy. In this analysis, we used the monitoring data in 13 years, from 1998 to 2011, for training models. Whereas 8 years measured data from 2011 to 2019 for validating models; therefore, the time span of the data used is satisfied.

6.5 | Statistical analysis

This section is devoted to evaluating the statistical significance of the model developed. The goal is to show that such model provided results significantly different from those of the other considered models.

The standard Wilcoxon rank-sum non-parametric (Haynes, 2013) test has been chosen to perform the statistical comparison. The metric selected has been MAE, as it was used as a cost function for optimizing all the methods.

Table 5 shows statistically significance in all cases, distinguishing two cases: those with $ps < 0.001$ (denoted by **) and those with $ps < 0.05$ (denoted by *).

7 | CONCLUDING REMARKS, LIMITATIONS, AND FUTURE WORKS

This research proposed and validated a new hybrid deep learning model, named CVOA-LSTM, for forecasting the deformation of the hydropower dam. A total of 260 monitoring samples spanning 21 years from 1998 to 2019 at the second-largest hydropower dam in Vietnam were used to verify the proposed model. Based on the finding, some concluding remarks are below:

1. LSTM is powerful for establishing a model to forecast the deformation of hydropower dam; however, it is challenging to determine the best structures, the learning rate parameter, and the dropout parameter; therefore, the optimization of these parameters must be carefully considered when using LSTM for dam behavior analysis in other research.
2. Based on the high forecasting performance of the proposed CVOA-LSTM model in this work, it can be concluded that proven CVOA is a good solution for



optimizing the three parameters of the proposed model autonomously.

3. The forecasting capability of the proposed CVOA-LSTM outperform that of the state-of-the-art machine learning algorithms (SMO-SVR, GP, M5', MLPNeuralNet, REPTree, RT, RF, RBFNeuralNet); therefore, the CVOA-LSTM is an alternative tool, which should be considered for the deformation forecasting of the hydropower dam.
4. One of the main limitations of this method is that LSTM networks take much time to be executed. When optimized with metaheuristics, this time can be extremely high and, for this reason, only fast metaheuristics or with few configurations should be used.
5. Furthermore, the use of transfer learning or deep reinforcement learning (Sorensen et al., 2020) should be considered due to the reduced size of the dataset analyzed, which can be considered a limitation of this work. Both learning paradigms would help the model to capture new features and find more complex relations.
6. Future research should consider other new optimization algorithms for searching optimized parameters of LSTM.
7. Future research should consider the application of other deep learning models, such as Gated Recurrent Units (GRU) or Temporal Convolutional Networks (TCN), given their usefulness for dealing with time series.

ACKNOWLEDGMENTS

This research is funded by Vietnam National Foundation for Science and Technology Development (NAFOS-TED) under grant number 105.08-2018.06. The authors also thank the Spanish Ministry of Economy and Competitiveness for the support under projects TIN2017-88209-C2 and PID2020-11795RB-C21. We also would like to thank Hoa Binh Hydropower Company for providing the periodically monitoring data and supporting us in collecting anomaly observations.

CONFLICT OF INTEREST

The authors declare no conflict of interest.

ORCID

Kien-Trinh T. Bui  <https://orcid.org/0000-0003-2265-7559>

José F. Torres  <https://orcid.org/0000-0001-7371-4352>

David Gutiérrez-Avilés  <https://orcid.org/0000-0002-6292-9873>

Viet-Ha Nhu  <https://orcid.org/0000-0003-1812-950X>

Dieu Tien Bui  <https://orcid.org/0000-0001-5161-6479>

Francisco Martínez-Álvarez  <https://orcid.org/0000-0002-6309-1785>

REFERENCES

- Alam, K. M. R., Siddique, N., & Adeli, H. (2020). A dynamic ensemble learning algorithm for neural networks. *Neural Computing with Applications*, 32(10), 8675–8690.
- Alba, E., Nakib, A., & Siarry, P. (2013). *Metaheuristics for dynamic optimization*. Springer Nature.
- Antes, H., & Von Estorff, O. (1987). Analysis of absorption effects on the dynamic response of dam reservoir systems by boundary element methods. *International Journal of Rock Mechanics and Mining Sciences & Geomechanics*, 25(3), 1023–1036.
- Belmokre, A., Santillan, D., & Mihoubi, M. K. (2021). Improved hydrostatic-season-time model for dam monitoring: Inclusion of a thermal analytical solution. *Lecture Notes in Civil Engineering*, 110, 67–78.
- Bui, K. -T. T., Bui, D. T., Zou, J., Van Doan, C., & Revhau, I. (2018). A novel hybrid artificial intelligent approach based on neural fuzzy inference model and particle swarm optimization for horizontal displacement modeling of hydropower dam. *Neural Computing and Applications*, 29(12), 1495–1506.
- Charte, F., Rivera, A. J., Martínez, F., & del Jesus, M. J. (2020). EvoAAA: An evolutionary methodology for automated neural autoencoder architecture search. *Integrated Computer-Aided Engineering*, 27(3), 211–23.
- Chen, S., Leng, Y., & Labi, S. (2020). A deep learning algorithm for simulating autonomous driving considering prior knowledge and temporal information. *Computer-Aided Civil and Infrastructure Engineering*, 35(4), 305–321.
- Dai, B., Gu, C., Zhao, E., & Qin, X. (2018). Statistical model optimized random forest regression model for concrete dam deformation monitoring. *Structural Control and Health Monitoring*, 25(6), e2170.
- De Sortis, A., & Paoliani, P. (2007). Statistical analysis and structural identification in concrete dam monitoring. *Engineering Structures*, 29, 110–120.
- Ding, L., Fang, W., Luo, H., Love, P. E., Zhong, B., & Ouyang, X. (2018). A deep hybrid learning model to detect unsafe behavior: Integrating convolution neural networks and long short-term memory. *Automation in Construction*, 86, 118–124.
- Divina, F., Torres, J. F., García-Torres, M., Martínez-Álvarez, F., & Troncoso, A. (2020). Hybridizing deep learning and neuroevolution: Application to the Spanish short-term electric energy consumption forecasting. *Applied Sciences*, 10(16), 5487.
- Du, S., Li, T., Yang, Y., & Horng, S. -J. (2020). Multivariate time series forecasting via attention-based encoder–decoder framework. *Neurocomputing*, 388, 269–279.
- Ezerskii, M., Skiba, S., & Bryukhov, S. (1990). Observations of unloading of the walls of the underground machine hall of the Hoa Binh hydroelectric station during construction. *Hydrotechnical Construction*, 24(5), 319–323.
- Ezersky, M., & Eppelbaum, L. (2017). Geophysical monitoring of underground constructions and its theoretical basis. *International Journal of Georesources and Environment-IJGE*, 3(3), 56–72.
- GSO. (2020). *General statistics office of Vietnam*. <https://www.Gso.Gov.Vn>
- Gurbuz, A. (2011). A new approximation in determination of vertical displacement behavior of a concrete-faced rockfill dam. *Environmental Earth Sciences*, 64, 883–892.



- Hariri-Ardebili, M. A., & Salazar, F. (2020). Engaging soft computing in material and modeling uncertainty quantification of dam engineering problems. *Soft Computing*, 24(15), 11583–11604.
- Haynes, W. (2013). Wilcoxon rank sum test. In W. Dubitzky, O. Wolkenhauer, K. H. Cho, & H. Yokota (Eds.), *Encyclopedia of systems biology*. Springer.
- Hochreiter, S., & Schmidhuber, J. (1997). Long short-term memory. *Neural Computation*, 9(8), 1735–1780.
- Hua, Y., Zhao, Z., Li, R., Chen, X., Liu, Z., & Zhang, H. (2019). Deep learning with long short-term memory for time series prediction. *IEEE Communications Magazine*, 57(6), 114–119.
- ICLA. (2012). Dam surveillance guide. International commission on large dams. *Technical Report*, B-158, Icold.
- Jeong, J. H., Jo, H., & Ditzler, G. (2020). Convolutional neural networks for pavement roughness assessment using calibration-free vehicle dynamics. *Computer-Aided Civil and Infrastructure Engineering*, 35(11), 1209–1229.
- Jiang, S., & Zhang, J. (2020). Real-time crack assessment using deep neural networks with wall-climbing unmanned aerial system. *Computer-Aided Civil and Infrastructure Engineering*, 35(6), 549–564.
- Kang, F., & Li, J. (2020). Displacement model for concrete dam safety monitoring via Gaussian process regression considering extreme air temperature. *Journal of Structural Engineering*, 146(1), 05019001.
- Kang, F., Liu, J., Li, J., & Li, S. (2017). Concrete dam deformation prediction model for health monitoring based on extreme learning machine. *Structural Control and Health Monitoring*, 24(10), e1997.
- Kao, C.-Y., & Loh, C.-H. (2013). Monitoring of long-term static deformation data of fei-tsui arch dam using artificial neural network-based approaches. *Structural Control Health Monitoring*, 20(3), 282–303.
- Lara-Benítez, P., Carranza-García, M., García-Gutiérrez, J., & Riquelme, J. C. (2020). Asynchronous dual-pipeline deep learning framework for online data stream classification. *Integrated Computer-Aided Engineering*, 27(2), 101–119.
- Li, M., Shen, Y., Ren, Q., & Li, H. (2019). A new distributed time series evolution prediction model for dam deformation based on constituent elements. *Advanced Engineering Informatics*, 39, 41–52.
- Li, Y., Bao, T., Gong, J., Shu, X., & Zhang, K. (2020). The prediction of dam displacement time series using STL, extra-trees, and stacked LSTM neural network. *IEEE Access*, 8, 94440–94452.
- Lin, C., Li, T., Chen, S., Liu, X., Lin, C., & Liang, S. (2019). Gaussian process regression-based forecasting model of dam deformation. *Neural Computing and Applications*, 31(12), 8503–8518.
- Liu, W., Pan, J., Ren, Y., Wu, Z., & Wang, J. (2020). Coupling prediction model for long-term displacements of arch dams based on long short-term memory network. *Structural Control and Health Monitoring*, 27(7), e2548.
- Luo, J., Zhang, Q., Li, L., & Xiang, W. (2019). Monitoring and characterizing the deformation of an earth dam in Guangxi Province, China. *Engineering Geology*, 248, 50–60.
- Martínez-Álvarez, F., Asencio-Cortés, G., Torres, J., Gutiérrez-Avilés, D., Melgar-García, L., Pérez-Chacón, R., Rubio-Escudero, C., Riquelme, J. C., & Troncoso, A. (2020). Coronavirus optimization algorithm: A bioinspired metaheuristic based on the COVID-19 propagation model. *Big Data*, 8, 308–322.
- Mata, J. (2011). Interpretation of concrete dam behaviour with artificial neural network and multiple linear regression models. *Engineering Structures*, 33(3), 903–910.
- Ni, F., Zhang, J., & Noori, M. N. (2019). Deep learning for data anomaly detection and data compression of a long-span suspension bridge. *Computer-Aided Civil and Infrastructure Engineering*, 35(7), 12528.
- Ni, L., Wang, D., Singh, V. P., Wu, J., Wang, Y., Tao, Y., & Zhang, J. (2020). Streamflow and rainfall forecasting by two long short-term memory-based models. *Journal of Hydrology*, 583, 124296.
- Ni, F., Zhang, J., & Noori, M. N. (2020). Deep learning for data anomaly detection and data compression of a long-span suspension bridge. *Computer-Aided Civil and Infrastructure Engineering*, 35(7), 685–700.
- Pereira, D. R., Piteri, M. A., Souza, A. N., Papa, J., & Adeli, H. (2020). FEMA: A finite element machine for fast learning. *Neural Computing and Applications*, 32(10), 6393–6404.
- Qin, X., Gu, C., Chen, B., Liu, C., Dai, B., & Yu, Y. (2017). Multi-block combined diagnosis indexes based on dam block comprehensive displacement of concrete dams. *Optik*, 129, 172–182.
- Ranković, V., Grujović, N., Divac, D., & Milivojević, N. (2014). Development of support vector regression identification model for prediction of dam structural behaviour. *Structural Safety*, 48, 33–39.
- Ranković, V., Grujović, N., Divac, D., Milivojević, N., & Novaković, A. (2012). Modelling of dam behaviour based on neuro-fuzzy identification. *Engineering Structure*, 35, 107–113.
- Ren, Q., Li, M., Song, L., & Liu, H. (2020). An optimized combination prediction model for concrete dam deformation considering quantitative evaluation and hysteresis correction. *Advanced Engineering Informatics*, 46, 101154.
- Rafiei, M. H., & Adeli, H. (2017). A new neural dynamic classification algorithm. *IEEE Transactions on Neural Networks and Learning Systems*, 28(12), 3074–3083.
- Rafiei, M. H., Khushefati, W. H., Demirboga, R., & Adeli, H. (2017). Supervised deep restricted boltzmann machine for estimation of concrete compressive strength. *ACI Materials Journal*, 114(2), 237–244.
- Rodríguez Lera, F. J., Rico, F. M., & Olivera, V. M. (2019). Neural networks for recognizing human activities in home-like environments. *Integrated Computer-Aided Engineering*, 26(1), 37–47.
- Ribeiro, L. S., Wilhelm, V. E., Faria, É. F., Correa, J. M., & dos Santos, A. C. P. (2019). A comparative analysis of long-term concrete deformation models of a buttress dam. *Engineering Structures*, 193, 301–307.
- Salazar, F., Toledo Á., M, O., E., & Suárez, B. (2016). Interpretation of dam deformation and leakage with boosted regression trees. *Engineering Structures*, 119, 230–251.
- Salazar, F., Morán, R., Toledo, M. Á., & Oñate, E. (2017). Data-based models for the prediction of dam behaviour: A review and some methodological considerations. *Archives of Computational Methods in Engineering*, 24(1), 1–21.
- Salazar, F., Toledo, M. A., Oñate, E., & Morán, R. (2015). An empirical comparison of machine learning techniques for dam behaviour modelling. *Structural Safety*, 56, 9–17.
- Shao, C., Gu, C., Yang, M., Xu, Y., & Su, H. (2017). A novel model of dam displacement based on panel data. *Structural Control Health Monitoring*, 25(1), e2037.



- Shi, Y., Yang, J., Wu, J., & He, J. (2018). A statistical model of deformation during the construction of a concrete face rockfill dam. *Structural Control and Health Monitoring*, 25(2), e2074.
- Sigtryggsdóttir, F. G., Snæbjörnsson, J. T., & Grande, L. (2018). Statistical model for dam-settlement prediction and structural-health assessment. *Journal of Geotechnical and Geoenvironmental Engineering*, 144(9), 04018059.
- Siqueira, H., Santana, C., Macedo, M., Figueiredo, E., Gokhale, A., & Bastos-Filho, C. (2020). Simplified binary cat swarm optimization. *Integrated Computer-Aided Engineering*, 28(1), 35–50.
- Sørensen, R. A., Nielsen, M., & Karstoft, H. (2020). Routing in congested baggage handling systems using deep reinforcement learning. *Integrated Computer-Aided Engineering*, 27(2), 139–152.
- Stojanovic, B., Milivojevic, M., Ivanovic, M., Milivojevic, N., & Divac, D. (2013a). Adaptive system for dam behavior modeling based on linear regression and genetic algorithms. *Advances in Engineering Software*, 65, 182–190.
- Su, H., Li, X., Yang, B., & Wen, Z. (2018). Wavelet support vector machine-based prediction model of dam deformation. *Mechanical Systems and Signal Processing*, 110, 412–427.
- Su, H., Wen, Z., Sun, X., & Li, H. (2017). Rough set-support vector machine-based real-time monitoring model of safety status during dangerous dam reinforcement. *International Journal of Damage Mechanics*, 26(4), 501–522.
- Tabari, M. M. R., & Sanayei, H. R. Z. (2018). Prediction of the intermediate block displacement of the dam crest using artificial neural network and support vector regression models. *Methodologies and Application*, 23, 9629–9645.
- Taormina, R., & Chau, K. W. (2015). ANN-based interval forecasting of streamflow discharges using the LUBE method and MOFIPS. *Engineering Applications of Artificial Intelligence*, 45, 429–440.
- Thurnhofer-Hemsi, K., López-Rubio, E., Roé-Vellvé, N., & Molina-Cabello, M. A. (2020). Multiobjective optimization of deep neural networks with combinations of Lp-norm cost functions for 3D medical image super-resolution. *Integrated Computer-Aided Engineering*, 27(3), 233–251.
- Torres, J. F., Galicia, A., Troncoso, A., & Martínez-Álvarez, F. (2018). A scalable approach based on deep learning for big data time series forecasting. *Integrated Computer-Aided Engineering*, 25(4), 335–348.
- Torres, J. F., Troncoso, A., Koprinska, I., Wang, Z., & Martínez-Álvarez, F. (2019). Big data solar power forecasting based on deep learning and multiple data sources. *Expert Systems*, 36(4), e12394.
- Torres, J. F., Gutiérrez-Avilés, D., Troncoso, A., & Martínez-Álvarez, F. (2019). Random hyper-parameter search-based deep neural network for power consumption forecasting. *Proceedings of the International Work-Conference on Artificial Neural Networks*, Gran Canaria, Spain (pp. 259–269).
- Torres, J. F., Hadjout, D., Sebaa, A., Martínez-Álvarez, F., & Troncoso, A. (2021). Deep learning for time series forecasting: A survey. *Big Data*, 9(1), 3–21.
- Tu, T., Zhu, F., Cao, A. W., He, L., & Ying, G. (2013). Application of Elm neural network in dam displacement early warning model. *Advanced Materials Research*, 864–867, 2363–2366.
- Vladimirov, V., Zaretskii, Y. K., & Orekhov, V. (2003). A mathematical model for monitoring the rock-earthen dam of the Hoa Binh hydraulic power system. *Power Technology and Engineering*, 37(3), 161–166.
- Wei, B., Chen, L., Li, H., Yuan, D., & Wang, G. (2020). Optimized prediction model for concrete dam displacement based on signal residual amendment. *Applied Mathematical Modelling*, 78, 20–36.
- World Health Organization (2021). <https://www.who.int/es/emergencies/diseases/novel-coronavirus-2019>.
- Wu, C. L., & Chau, K. W. (2013). Prediction of rainfall time series using modular soft computing methods. *Engineering Applications of Artificial Intelligence*, 26(3), 997–1007.
- Wu, R. T., Singla, A., Jahanshahi, M. R., Bertino, E., Ko, B. J., & Verma, D. (2019). Pruning deep convolutional neural networks for efficient edge computing in condition assessment of civil infrastructures. *Computer-Aided Civil and Infrastructure Engineering*, 34(9), 774–789.
- Xi, G. -Y., Yue, J. -P., Zhou, B. -X., & Tang, P. (2011). Application of an artificial immune algorithm on a statistical model of dam displacement. *Computers & Mathematics with Applications*, 62(10), 3980–3986.
- Xu, J., Gui, C., & Han, Q. (2020). Recognition of rust grade and rust ratio of steel structures based on ensemble convolutional neural network. *Computer-Aided Civil and Infrastructure Engineering*, 35(10), 1160–1174.
- Yang, D., Gu, C., Zhu, Y., Dai, B., Zhang, K., Zhang, Z., & Li, B. (2020). A concrete dam deformation prediction method based on LSTM with attention mechanism. *IEEE Access*, 8, 185177–185186.
- Zhang, A., Wang, K. C. P., Fei, Y., Liu, Y., Chen, C., Yang, G., Li, J. Q., Yang, E., & Qiu, S. (2019). Automated pixel-level pavement crack detection on 3D asphalt surfaces with a recurrent neural network. *Computer-Aided Civil and Infrastructure Engineering*, 34(3), 213–229.
- Zheng, D., Cheng, L., Bao, T., & Lv, B. (2013). Integrated parameter inversion analysis method of a CFRD based on multi-output support vector machines and the clonal selection algorithm. *Computers and Geotechnics*, 47, 68–77.
- Zou, J., Bui, K. -T. T., Xiao, Y., & Doan, C. V. (2018). Dam deformation analysis based on BPNN merging models. *Geo-Spatial Information Science*, 21(2), 149–157.

How to cite this article: Bui, K. -T. T., Torres, J. F., Gutiérrez-Avilés, D., Nhu, V-Ha, Bui, D. T., & Martínez-Álvarez, F. Deformation forecasting of a hydropower dam by hybridizing a long short-term memory deep learning network with the coronavirus optimization algorithm. *Comput Aided Civ Inf*. 2021;1–19. <https://doi.org/10.1111/mice.12810>

APPENDIX

This appendix is included to show visual information for the methods used to assess the performance of CVOA-LSTM.

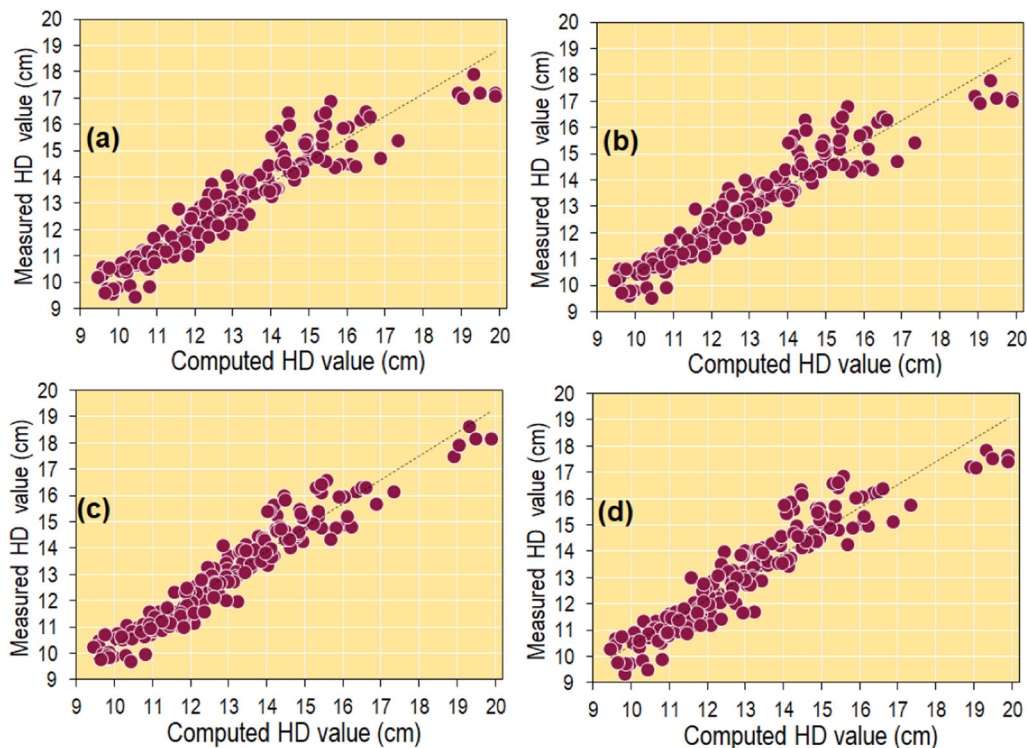


FIGURE A1 R^2 of the HD models on the validation dataset: (a) the sequential minimal optimization for support vector regression (SMO-SVM) model, (b) the Gaussian process (GP) model, (c) the M5 model tree (M5') model, and (d) the MLPNeuralNet model

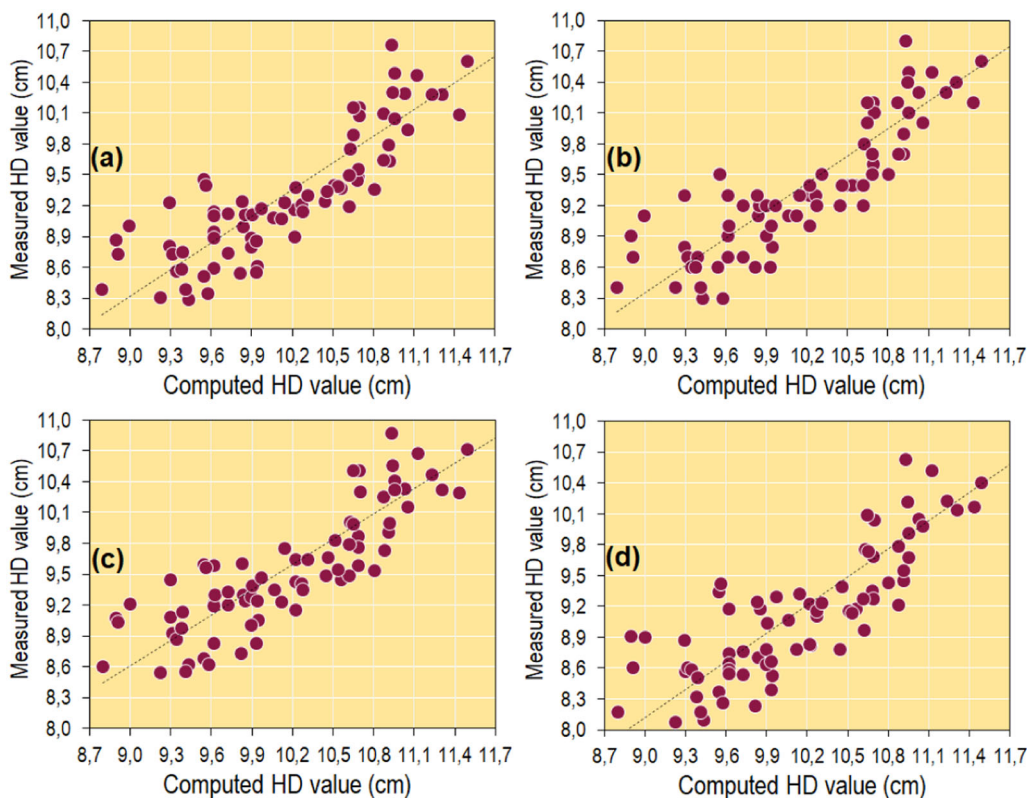


FIGURE A2 R^2 of the HD models on the test dataset: (a) the SMO-SVM model, (b) the GP model, (c) the M5' model, and (d) the MLPNeuralNets model

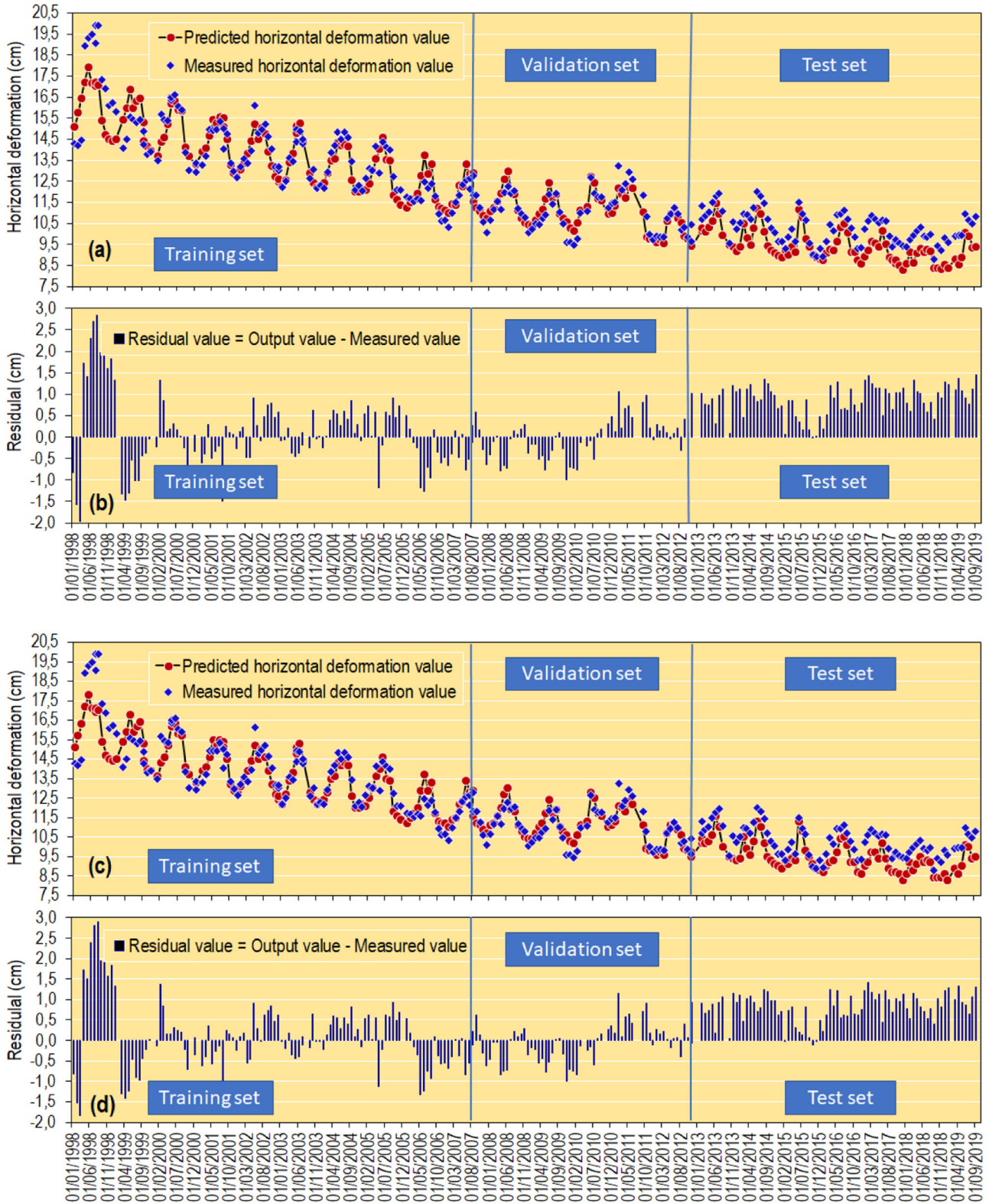


FIGURE A3 Predicted HD values versus measured HD values and the residual of the SMO-SVM model (a,b) and the GP model (c,d). The M5' (e,f) and the MLPNeuralNets model (g,h)

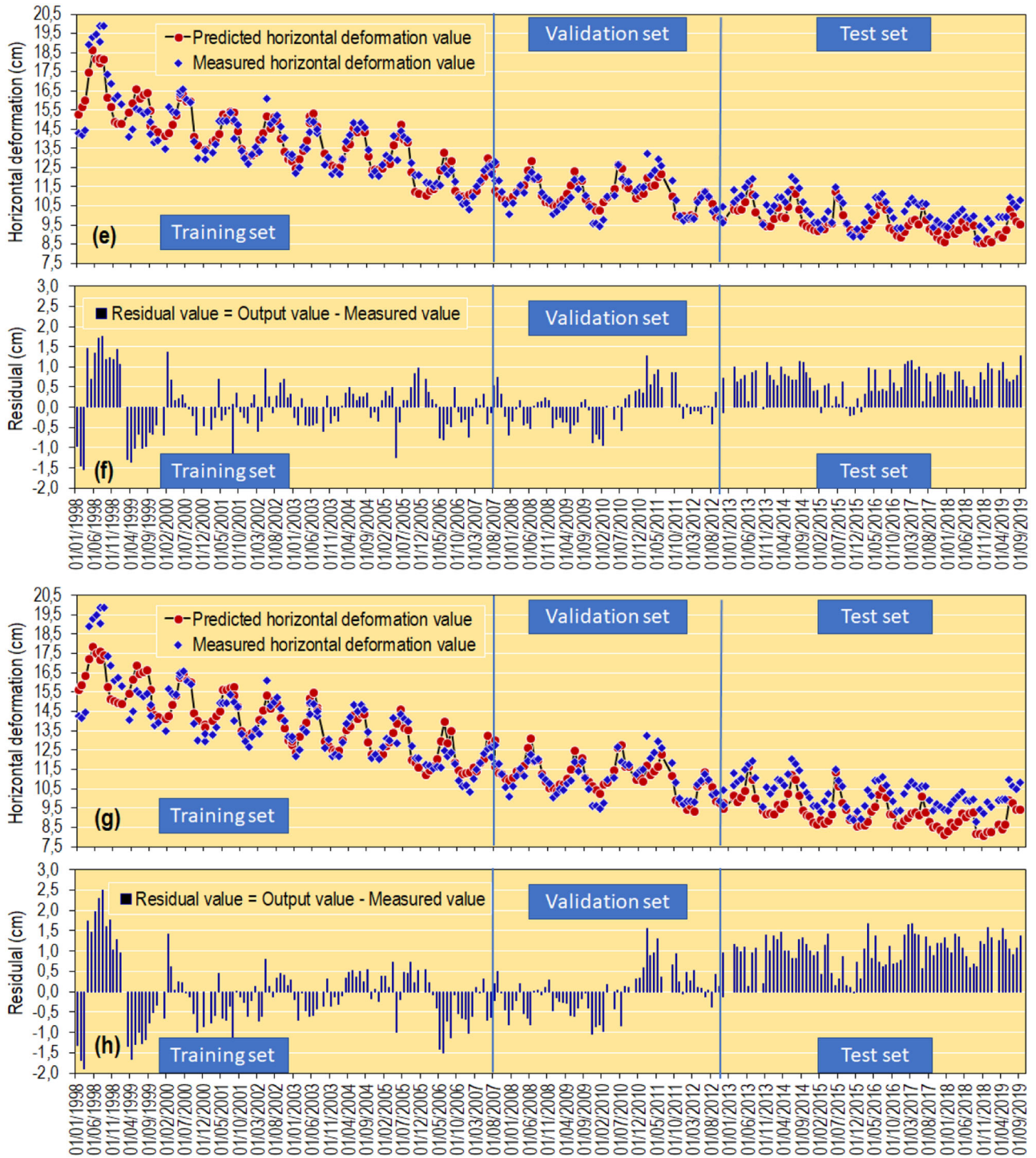


FIGURE A3 Continued